Romanian Reports in Physics, Vol. 62, No. 3, P. 594–609, 2010

Dedicated to the 50th LASER Anniversary
(LASERFEST-50)

LASER PROCESSING AND CHARACTERIZATION WITH FEMTOSECOND LASER PULSES

M. ZAMFIRESCU[1], M. ULMEANU[1], F. JIPA[1], I. ANGHEL[1], S. SIMION[1], R. DABU[1], I. IONITA[2]

[1]*National Institute for Laser, Plasma and Radiation Physics INFLPR-Bucharest, Atomistilor 409, 077125 Magurele, Romania, E-mail: marian.zamfirescu@inflpr.ro*
[2]*Bucharest University, Faculty of Physics, Atomistilor 405, 077125 Magurele, Romania*

(Received June 16, 2010)

Abstract. The nonlinear interaction of femtosecond laser pulses with matter allows the physical and chemical modification of materials at micro and nano-scale. We present an experimental set-up for direct laser structuring by ultra-short laser pulses using nonlinear laser absorption on various materials such as metallic film, transparent photoresists, ceramics etc. A microscope for laser processing and laser characterization was designed and constructed to be coupled with various laser systems. The laser workstation was designed to be used for different laser structuring techniques such as laser ablation, two-photon photopolymerization (TPP), laser induced forward transfer (LIFT), near field laser lithography (NFLL). The configuration of the system allows also the spectroscopic characterization of materials by two-photon excitation (TPE).

Key words: laser direct writing, 3D laser microlithography, laser patterning, femtosecond laser, two-photon photopolymerization, two-photon excitation spectroscopy.

1. INTRODUCTION

In fifteen years of development of laser technology, the lasers were involved in almost all scientific and technical domains from industry, medicine, defence etc. [1-3]. The latest challenges of lasers applications are related to the use of lasers for micro and nanostructuring [4]. Fabrication technologies on the micro and nanometer scale are becoming more and more important from the viewpoint of industrial applications, for example, high-resolution lithography for the manufacture of high-density recording media, high-resolution displays or high-sensitivity biomolecule sensor arrays. Electron beam lithography, ion beam lithography, X-Ray lithography, are techniques with and excellent feature size control [5, 6]. However, these are characterized by low throughput, and high sample cost. Conventional photolithography remains a large scale fabrication technology due to its capability for large-area fabrication. Because the minimum feature size is

limited by optical diffraction, submicrometer structures are currently created by Deep UV (DUV) at 248 nm, or Extreme UV (EUV), which is considered the next-generation lithography technology using the 13.5 nm wavelength [7]. Because such technology requires complex vacuum optics, the cost of these remains prohibitive.

Femtosecond lasers could offer an alternative to the other micro and nano-structuring method. Due to the high pulse intensity, the most of nonlinear effects are easily induced in materials even at low energies per pulse. The nonlinear two or multiphoton absorption induce physical and chemical modifications of materials at micro and nano-scale. Thus, the fabrication of micro-devices using lasers is possible by means of controlled modification of the materials under light irradiation. When an ultrafast laser beam with pico- or femtosecond pulse duration is tightly focused on the surface of a solid sample or inside a transparent material, if the laser fluence exceeds a certain threshold, a small volume of material is ablated, or fotochemical reactions are induced, leaving behind patterns with micrometer or sub-micrometer dimensions [8-11]. Due to the long heat-diffusion time of almost all of materials compared to the pulse duration of commercially available femtosecond laser systems, the adjacent surface of the processed area remains almost unaffected. This characteristic makes the laser processing with ultrafast lasers to become a processing technique suitable for configuration of microstructures both in 2D at the surface of materials, or 3D in the volume of transparent materials. Various materials such as metallic films, ceramics, polymers, and transparent glasses can be laser processed with application on fabrication of microelectronics circuits, microsensors, or other MEMS. In this paper we present the techniques and the experimental set-up used for laser micro and nanostructuring. A laser workstation for laser direct-writing (LDW) was designed and built. Different techniques such as laser ablation, two-photon photopolymerization (TPP), laser induced forward transfer (LIFT), near field laser lithography (NFLL), was demonstrated. The system was also configured for spectroscopic characterization of materials by two-photon excitation (TPE) with application on high resolution microscopy.

2. WORKSTATION FOR LASER DIRECT-WRITING

A microscope for laser direct-writing was developed for computer controlled micro-structuring of materials. It was conceived in a modular configuration to satisfy any experimental requirement. For example, working at a different radiation wavelength is possible by simply replacing few modules or components. The main modules are: the laser beam delivery module; attenuation module; the focusing optics; the sample translation stages in XYZ; the visualisation system with video camera; the confocal module for light collection from sample for signal analysis.

In our experiments, different laser sources were coupled with the LDW workstation. For laser ablation of almost all of materials, laser beam with energy of more than tens of nano-Joules up to micro-Joules is required. In this case, an amplified femtoseconds laser system Clark CPA-2101 we use. The laser emits femtoseconds pulses with 200 fs pulse duration, at 2 KHz repetition rate and 775 nm wavelength. The maximum laser energy is about 0.6 mJ per pulse. The second harmonic can be generated by a BBO nonlinear crystal at 387 nm with more than 40% conversion efficiency. Laser ablation was also performed with the same microscope at 1064 nm and 532 nm emitted from a Nd:YAG laser with 400 ps pulse duration at 1 up to 10 Hz. High repetition rate experiments were performed with two different femtoseconds laser oscillators at 80 MHz: a Spectra Physics - Tsunami, tunable in the spectral range from 750 to 850 nm, with 80 fs pulse duration, and a Femtolasers-Synergy Pro oscillator at 790 nm, 10 fs pulse duration, and 100 nm spectral band width. The beam delivery optics is interchangeable and can be easily replaced with optics adapted for the working wavelengths.

The laser energy can be continuously and precisely attenuated with an attenuation system composed by a motorised half wave plate placed in front of a Glan polarizer providing a 300:1 extinction rate. In the case of extremely short pulse duration, a reflective polarizer is used for avoiding the temporal stretching of femtoseconds pulses due to the dispersion introduced by bulk material. A dielectric mirror reflects the laser beam to the focusing optics and transmits the other wavelength to the visualization system and to the characterisation module.

The focusing optics can be different microscope objectives or lenses with a wide range of numerical aperture, adapted to a specific application. Different thread standards can be used via available thread adapters. For laser ablation of very small features, a 100X Mitutoyo microscope objective with numerical aperture NA = 0.5 and 12 mm working distance is used for focusing the femtosecond laser. Such long working distance allows also the focusing of the laser beam deeply in the volume when transparent materials are processed. Immersion oil Zeiss microscope objective with 1.4 numerical aperture in used for laser processing or characterization of materials at submicron resolution. However, its reduced working distance of about 0.15 mm limits the field of applications.

The sample is translated by XYZ motorized stages and piezo drivers. Two different translation stages are used. A Nanocube stage (Thorlabs) has a total travel range of 4×4×4 mm^3 with hundreds of nm accuracy. The embedded piezo stage has 20 μm travel range per each axis and accuracy down to 5 nm. For longer travels, linear stages with 50 mm maximum travel are used. The maximum translation speed is 2 mm/s. The translations are computer controlled for generating any path according to a computed design. The sample focusing is done by the visualization system with CCD and a 200 mm tube lens. The resolution of the visualization system is better than 1 μm when the 100× objective microscope is used.

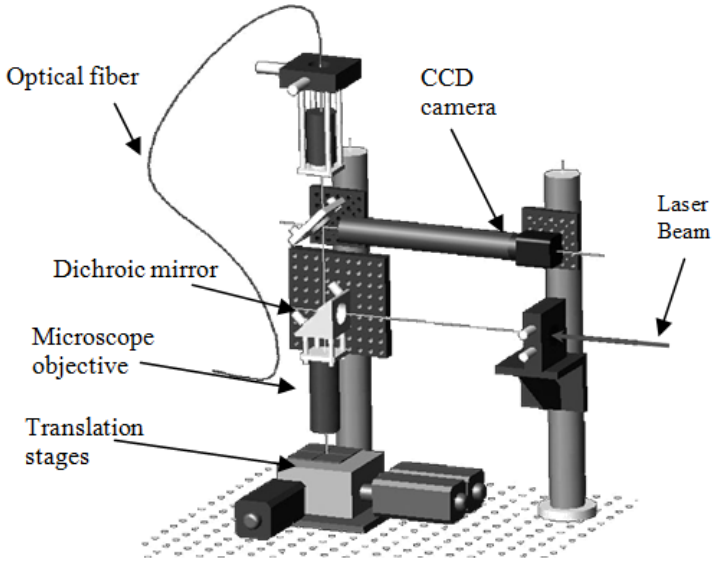

Fig. 1 – The design of laser direct writing workstation.

The same focusing objective is used for light collection. The optical signal is collimated and sent to the upper part of the microscope trough the dichroic mirror. The light is coupled by a second focusing lens to an optical fiber in a confocal configuration. The collected optical signal is transmitted by an optical fiber to be measured or analyzed by a photomultiplier or spectrometer.

Dedicated software was realized for controlling the laser processing of samples. Common geometries such as parallel lines, grids, interdigitated structures, periodical structures of dots in rectangular or hexagonal symmetry, are included in a predefined library. More complex designed structures can be imported from files in bitmap format for 2D surface structuring, or in STL format in the case of 3D structuring of transparent materials. The STL is a standard format commonly used in rapid prototyping.

Using the above described microscope, we demonstrated several applications of femtoseconds laser on microprocessing and for optical spectroscopy characterization.

3. FEMTOSECOND LASER ABLATION AS A DIRECT WRITING TECHNIQUE OF MICROSTRUCTURES

When an infrared femtosecond laser beam is tightly focused at the surface of a material, due to the very high laser power density (GW-TW/cm^2), multiphotonic absorption followed by avalanche ionization and laser ablation can be induced in a volume smaller than the focused spot size. The temperature of the materials at the

centre of the focused spot reaches rapidly very high temperatures, and the material is removed by ablation. Since the laser pulse duration is very short compared to the thermal diffusion time, the adjacent surface of the irradiated area remains unaffected. Therefore, femtoseconds lasers can be used for precisely processing of almost any kind of materials, such as metallic films, ceramics, polymers. Compared to the classical lithography techniques, laser ablation is a direct writing method, no mask is required, and no corrosive chemicals are used, so it is an environmental friendly technique. It is a suitable method for producing microstructures for various electronic devices, such as interdigital capacitors, were fine electrodes has to be produced.

The fines of the fabricated structures can be controlled by the focusing optics and the laser energy deposited to the material. The following relations describe the dependence of the size of the ablated spot with the laser fluence:

$$d(F) = \frac{d_0}{\sqrt{2}} \sqrt{\ln(F / F_{th})}\,, \tag{1}$$

where d_0 is the focused beam diameter given by the laser wavelength – λ, beam quality factor – M^2, and the focusing numerical aperture – NA:

$$d_0 = \frac{2M^2\lambda}{\pi NA} \approx \frac{\lambda}{NA}\,. \tag{2}$$

Figure 3a shown the principle of laser processing with resolution below the size of the focused laser spot d_0. When the laser intensity is kept just above the ablation threshold, the material modification takes place only in the center of the focused beam, where the laser fluence exceeds the intensity of modification threshold. Therefore, when the laser beam is tightly focused in a very small spot and the intensity is well controlled and kept at threshold, laser processing is possible even below the optical diffraction limit. In Fig. 3b is shown the dependence given by Eq.1, of the diameter d of the ablated spot in function of laser intensity for an experimental case of a focuses beam diameter of $d_0 = 2$ μm.

Laser ablation was performed on different materials. In Figs. 3 different films processed by focused femtosecond laser beam are shown. The structured materials in Figs. 3a and b are gold films with 100 nm thickness deposited on glass substrate, and a multilayer Co/Cu/Co structure deposited on Si substrate, in Fig. 3c. For laser processing, the 200 fs radiation at 775 nm from Clark CPA2101 laser was coupled with the processing microscope. The focusing optics was a 100× microscope objective with NA = 0.5. The laser fluence is kept just above the ablation threshold in order to obtain small features on sample surface. Periodical structures such as holes, parallel lines, or grids were created by predefined structures library from the software. The parallel lines were created by translating

the sample with the scanning speed of 0.2 mm/s. The width of the laser structured electrodes is below 1 μm. The period of the structures was 2 μm. At this level of structuring, the periodicity of the structures is affected by the limited positioning accuracy of the translation stage, as observed in Fig. 3b. With piezo translation stages more accurate structuring can be realized, however the travel range is limited to hundreds of micrometers even in the case of the most outstanding piezo drivers available.

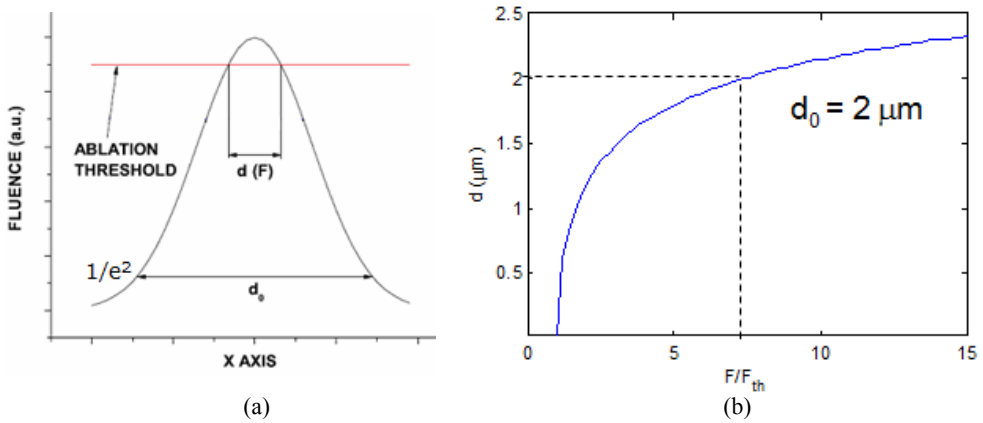

Fig. 2 – a) The principle of laser ablation below the diffraction limits; b) dependence of the ablated spot diameter in function of the laser fluence for a focused beam diameter of $d_0 = 2$ μm.

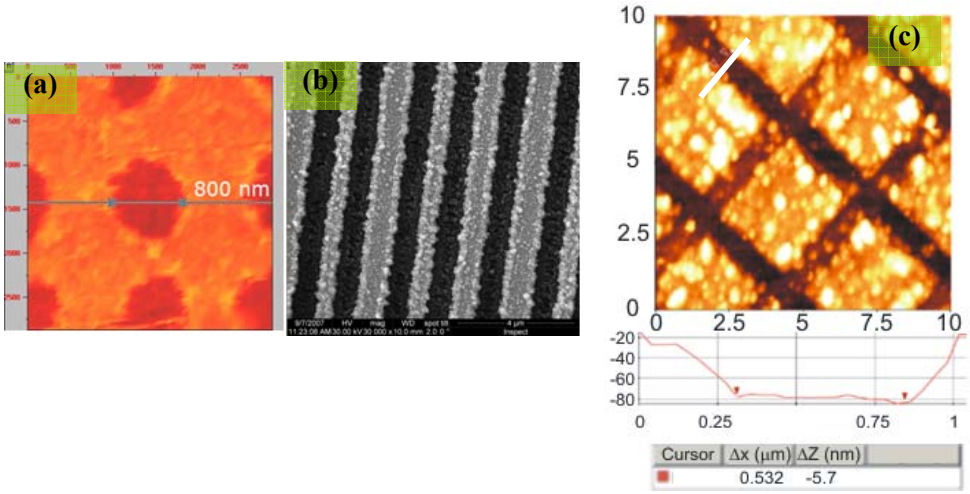

Fig. 3 – Thin films structured by femtosecond laser beam: a) AFM image of holes ablated in a 100 nm thick gold film; b) SEM image of gold electrodes on glass substrate; c) grid structure in a multilayer Co/Cu/Co film. The width of ablated lines is about 530 nm.

The grids structures on multilayer films are presented in Fig. 3c. The lines in X and Y direction were processed by scanning the sample with the speed of 0.3 mm/s. The width of the ablated lines is 530 nm, below the diffraction limit.

Many of devices for microelectronics are commonly produced by classical lithography. In some applications, such as high frequency microwaves or millimeter wave (MMW) devices, the geometrical dimensions of the circuit layout reach the limits of classical photolithography. So, the laser ablation could be a valuable technique to process such devices [12].

4. 3D STUCTURING BY TWO-PHOTON PHOTOPOLYMERIZATION IN PHOTORESITS

The nonlinear effect of two-photon photopolymerization (TPP) in photoresists was intensively used in the last years for developing the micro-stereo-lithography technique [13-17]. 3D microstructures can be realized by NIR femtosecond lasers processing in materials which are normally transparent to the NIR radiation. When a femtosecond laser beam is focused in the volume of a transparent photorezist, due to the high peak intensity in the beam waist, a high probability of two-photon [18] or multiphoton absorption occurs [19].

A large series of photoresists such as SU-8, Ormoces, KMPR, PMMA, etc. has the maximum of the absorption band in the UV-blue spectral range. In such photopolymers the two-photon absorption of NIR femtosecond laser pulses induces photochemical reactions and then photopolymerization, just like in the case of a single UV photon absorption. In contrast with the single photon processing, the two-photon absorption occurs in a very tiny volume of material, at the center of the focused spot, were the laser intensity exceed the photopolymerization threshold (Fig. 4).

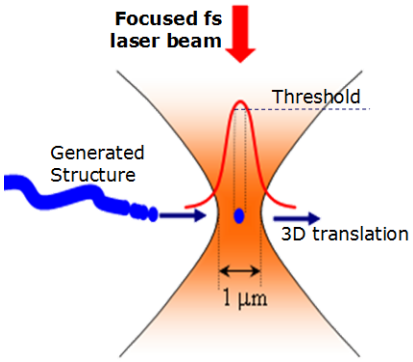

Fig. 4 – The schematic of 3D microphotolithography by TPP.

If the laser fluence is keeped low enough, small features can be created with resolution down to tens of nm's [20,21]. Following the rapid prototyping algorithms practically any 3D computer designed geometries can be fabricated. After laser irradiation, the polymerized sample is rinsed in a specific solvent for removing the non irradiated material. Then, complex microstructures are produced. However, in applications such as micro/nanophotonics or microfluidics, some designs are difficult to be realized because of the limited aspect-ratio of the structures, shrinkage and deformation of the polymerized structure, or collapsing of the structure on the substrate after removal of sample from the solvent.

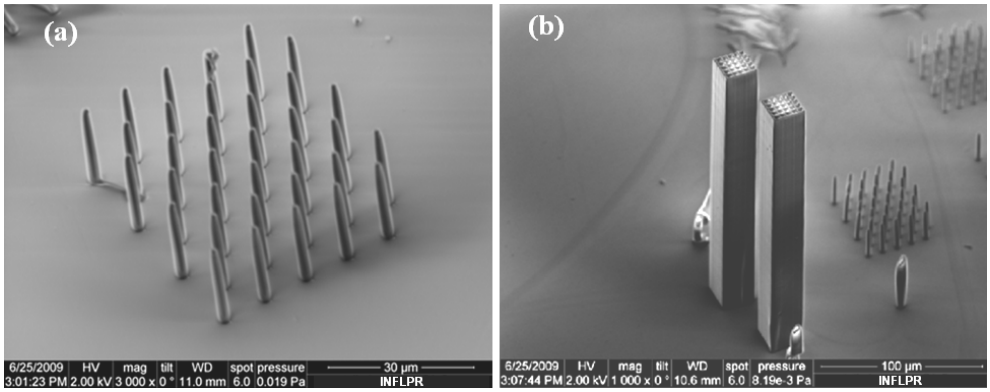

Fig. 5 – Structures realized by TPP in SU-8 with aspect-ratio of 10:1; a) pillar structures 20 μm high; b) 3D blocks 200 μm high.

In Fig. 5, high-aspect-ratio structures in SU-8 photoresist are presented. For TPP, the femtosecond oscillator Synergy Pro working at 80 MHz repetition rate was used. The laser emits pulses with duration of 10 fs. Nevertheless, much longer pulse duration is expected on the sample, about 200 fs, due the large spectral bandwidth of the laser and the GDD introduced by all the glasses in the optical path, including the focusing optics. An optical compressor with prisms can be used in order to pre-compensate the time dispersion on the optical path. The focusing optics was a microscope objective with 0.5 *NA*. In these exposure conditions the photopolymerized voxel has an ellipsoidal shape with 2 μm in diameter and about 7 μm along the Z axis. From the scanning speed we can estimate the exposure time of about 150 ms per voxel and per single scan.

Vertical structures such as columns or blocks are realised in photopolymers. From the SEM images in Fig. 5a we estimated the dimensions of the columns. Their height is 20 μm and the diameter is 2 μm. Then, a 10:1 aspect ratio was produces for pillars structures. Also, higher structures can be produced. In Fig. 5b is presented the SEM image of vertical blocks as high as 200 μm with 20×20 μm^2 squared base. These structures were built in woodpile geometry with distance

between adjacent planes of 2 μm, less that the voxel height, in order to obtain a continuum and smooth vertical wall. From SEM image the dimensions of the blocks reveal a 10:1 aspect ration.

The demonstrated TPP technique can be used for fabrication of photonic devices such as photonic crystals, optical couplers, diffractive elements, or 3D structures for microfluidics, scaffold for tissue engineering or other MEMS.

5. FEMTOSECOND LASER INDUCES FORWARD TRANSFER

Laser Induced Forward Transfer (LIFT) is a technique that can be challenging to the conventional etching techniques because it is not necessary to use complicated photolithographic processes. This technique is in particular interesting when very small quantity of material has to be deposited to a substrate. LIFT was initially used for metals patterns depositions [22, 23]. Afterward, it was shown that many kinds of materials such as semiconductors, polymers, or even biological material can be transferred [24-29]. The material to be transferred is initially deposited in thin films on a transparent substrate named donor substrate, or "ribbon" (transparent at laser radiation used for LIFT process). Usually, but not necessarily, a very thin metallic layer is deposited as buffer between the donor substrate and the film to be transferred. The donor sample, is placed parallel and at a short distance with another substrate (virtually any material), which is the acceptor. The donor film is irradiated backward with a pulsed laser, like in Fig. 6.

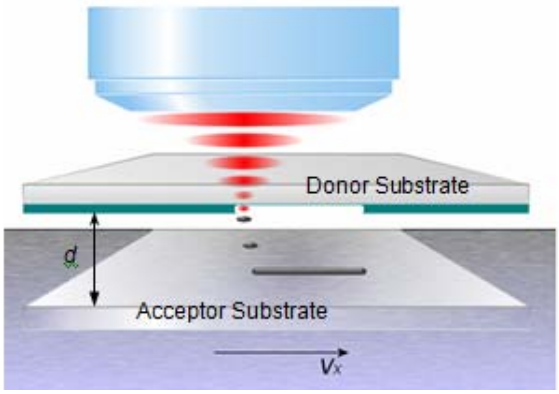

Fig. 6 – The schematic of LIFT principle.

The laser is focused on the donor thin film at the interface with the donor substrate. Then, a small amount of buffer material is ablated and transformed in gaseous faze. This gas expands pushing forward the rest of the material which is

projected to the acceptor substrate. If the parameters are correctly chosen, the ejected material is deposited to the acceptor's surface. The role of the buffer layer is only to protect the material to be transferred and is used especially in the case of organic materials susceptible to be affected by a direct exposure to the laser beam. Otherwise, in absence of a buffer layer, the material itself can be vaporized at the interface with the donor substrate, the pressure of the created gas transferring a small quantity of material from a substrate to another.

In LIFT experiments some of the parameters like distance *d* between donor film and acceptor substrate, or laser fluency, has to be investigated in order to find the optimal processing conditions for deposition a certain material. In our LIFT experiment we demonstrate the transfer of a polymer material, an ORMOCER photoresist, using our laser processing workstation. The polymer layer was deposited by spin coating directly on glass substrate, without any buffer layer. The distance between donor and acceptor is fixed at 15 μm. Series of 5×5 pixels are created by single pulses, shot by shot. The laser source was the Clark CPA-2101 laser, with 200 fs pulse duration and 775 nm wavelength, externally triggered for single shot experiments. The sample was translated from a pixel to another by a computer controlled translation stage. The distance between pixels was 50 μm. The laser was focused to the donor layer by a 75 mm focusing lens with about 25 μm focus spot diameter. The energy per pulse was varied from 2.5 to 7.5 μJ.

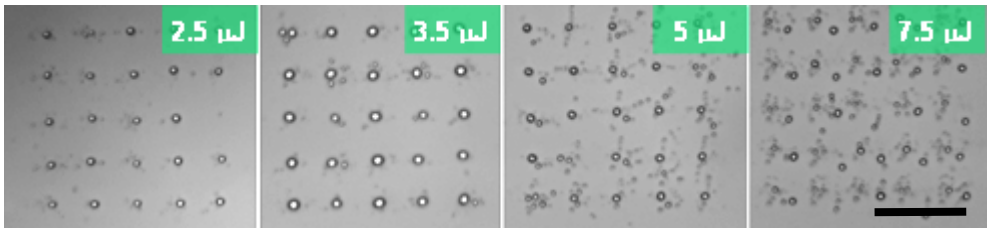

Fig. 7 – Morphology of LIFT generated microstructures at different laser energy. The scale bar is 100 μm.

Figure 7 shows the optical images of the structures as transferred to the acceptor substrate at different pulse energies. The quality of the obtained structures strongly depends on the pulse energy. At highest pulse energy used, non uniform droplets results, sparse on the donor surface. Decreasing the pulse energy the transferred droplets remain well defined.

The smallest size of the droplets obtained in these experimental conditions was about 2 μm. Even smaller structures, such as nanodroplets, can be transferred [30], or at opposite an entire microstructure or a microdevice ca be deposited by LIFT [31]. Then, this technique can be efficiently used as a microprinting method, and is also demonstrated in our experimental set-up.

6. NEAR FIELD LASER LITHOGRAPHY

Micromachining using short (picosecond-ps) and ultra short (femtosecond-fs) has been widely investigated in recent years because of its potential for high precision and almost melt-free processing of materials. Most of the applications, however, are limited to microscales or little below the micrometer size, which results from the optical diffraction limit associated with conventional optics [32]. Near-field optics is one of the most promising techniques to circumvent the optical diffraction limit and thus to apply these techniques to nanoscience and nanotechnology which deal with structures with features less than 100 nm [33-36].

Recent experiments have shown that light enhancement can produce a hot spot, resulting in the formation of a small pit on a silicon substrate using femtosecond or nanosecond pulsed lasers [37, 38]. Near-field enhancement in the vicinity of nanometer-size particles is capable of producing nanostructuring of large areas in a parallel processing, without complicated focusing and scanning systems. In this configuration, the enhanced field is confined in an area defined by the particle size to produce nanosize modification on a substrate. The optical field enhancement mechanism can be due to the lens effect or Mie's scattering depending on the particle size when transparent dielectric particles are used [39, 40]. Using this method nanoholes array are fabricated by laser irradiation mediated by hexagonally arrayed polystyrene particles [41].

Figure 8 presents the numerical simulation of the propagation of the light at 532 nm in vicinity of microsphere with 3 μm in diameter. In this simulation, the Maxwell equations are numerically resolved by finite difference time domain algorithm (FTDT). The Rsoft package from Rsoft Design was used for this calculation.

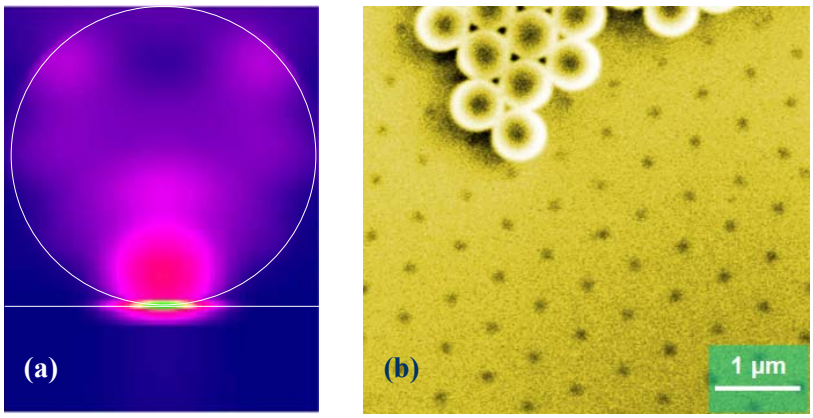

Fig. 8 – Near field laser lithography: a) FDTD simulation of optical field enhancement underneath a microsphere; b) laser patterning of a glass substrate by NFLL.

Experimentally, for obtaining a monolayer of microfocusing objects, a droplet of colloidal particles is placed on the substrate using a pipette. Following the water evaporation, layers of colloidal particles are self-assembled on the surface. Further details of the self-assembly process can be found elsewhere [42]. The substrates covered with a well organized monolayer of colloidal particles were irradiated with a single laser pulse width of 400 ps at a wavelength of 532 nm.

Figure 8b presents the SEM image of a glass substrate after laser irradiation in near-field regime. The optical enhanced field at the interface of spheres with the substrate leads to laser ablation in the very small volume of the glass substrate. Simultaneously, the spheres are removed from de surface. A pattern of nanoholes with diameter of 100 nm remain of the surface.

For the 400 ps laser pulse duration the ablation of metals is still a thermal process. Optical energy is absorbed by the free electrons and transfered to the lattice by electron-phonon coupling. The electron-phonon relaxation time τ of metals is of the order of a few picoseconds [43]. After this relaxation time the electrons are in thermal equilibrium with the lattice. If the applied fluence is above certain threshold fluence, the lattice temperature exceeds the melting point and the material will be removed by evaporation and melt expulsion.

7. TWO-PHOTON EXCITED SPECTROSCOPY

The Two-Photon Excited Photoluminescence (TPE-PL) or SHG signal we measured using the previously described microscope. When the laser source is a femtoseconds pulsed laser, and the laser fluence is below the threshold of any damaging effects, the nonlinear absorption induces two-photon excited emission [44-46]. In the case of focusing optics with high numerical aperture, the emitting volume can be with size less than the dimension of the excitation laser spot, even much below the diffraction limit. This behavior is commonly used in high resolution microscopy using TPE effect.

Characterization capabilities were added to our processing workstation. A confocal configuration is used in order to couple the signal from the laser irradiated sample, via an optical fiber, to a measuring device, such as a spectrometer, phototube, or an avalanche photodiode (Fig. 9).

The focusing optics, L1, has also the function of a collection lens collimating the signal to the measurement module at the top of the microscope. The collimated emission from the sample is coupled by a 40 mm lens, L2, to a multimode optical fiber. These two lenses, the collection microscope objective and the coupling lens, form together a confocal system in infinite conjugate configuration [47]. The ratio between the magnifications of the two lenses gives the resolution of the confocal system. For our 0.5 NA microscope objective, having 2 mm focus, a 1:20 ration is obtained. If in the focus plane of the coupling lens a 20 μm pinhole is placed, or optical fiber with similar core diameter is used, the spatial resolution of the confocal microscope is about 1 μm.

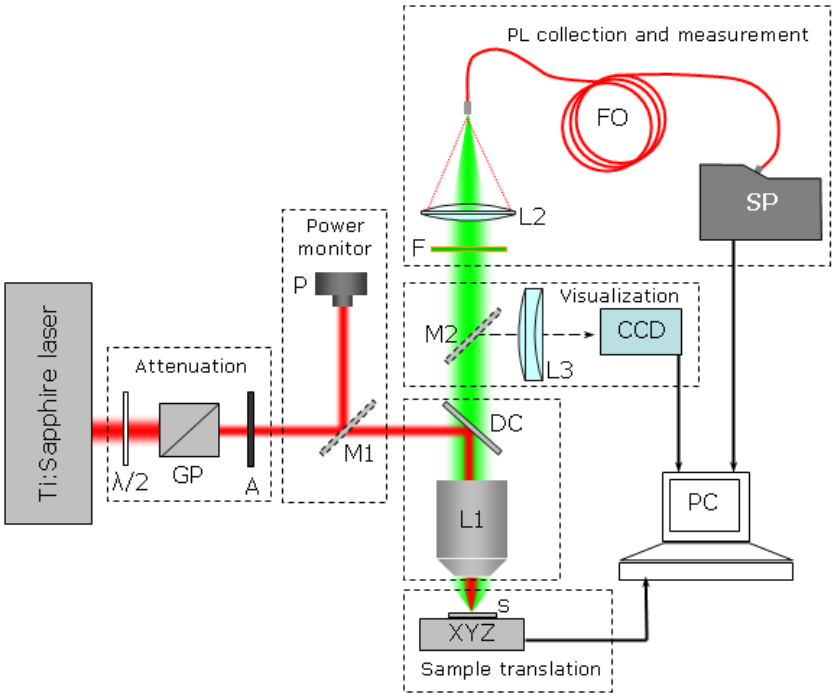

Fig. 9 – Experimental set-up for two-photon excited photoluminescence: GP – glan polarizer; A – neutral density filters; P – powermeters ; DC – dichroic mirror; L1–20× focusing lens; S – sample; XYZ – translation stage; L2 – coupling lens; FO – optical fiber; SP – spectrometer; L3 – imaging lens; CCD – video camera.

Better resolution can be obtained by femtoseconds laser due to the TPE effects. In order to separate the PL signal from the scattered laser, in front of the coupling lens a dichroic mirror is used as beam delivering optics. This mirror is placed in a kinematic mount for rapid replacement when a different wavelength of the laser source in used. When working with a Ti:Sapphire laser, the dichroic mirror has the cutoff wavelength at $\lambda > 650$ nm with transmission about 90% of the TPE-PL signal and 98% reflection of the laser wavelength at 800 nm. The optical signal can be analyzed by an Ocean Optics spectrometer HR4000+. In this case the integration time can be as long as few seconds for low emitting sample.

Scanning microscopy can be performed with our system using the fast piezo scanners embedded in the Nanocube translation stage. In this case a more sensitive detector is required in order to reduce considerably the measurement integration time. For our system a PMMC detector can be used for spectrally integrated measurement. Fast spectral measurements are done synchronously with the translation of the sample by an Andor spectrometer with iDus ICCD camera at few ms integration time.

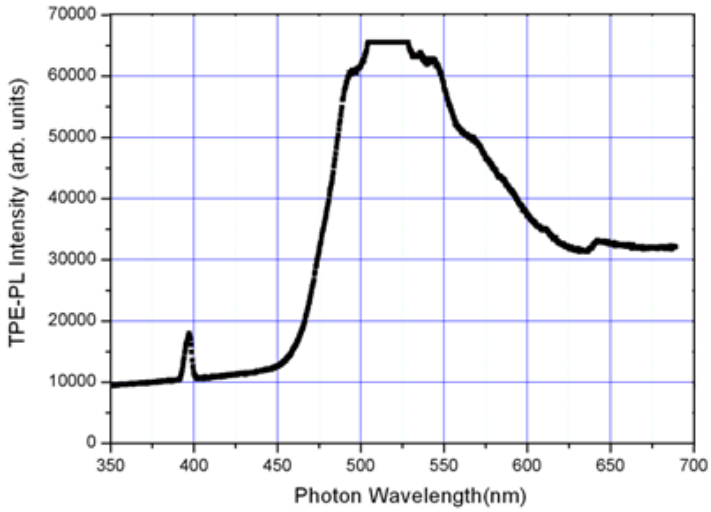

Fig. 10 – The emission of complex organic thin film sample, obtained by 2-photon excitation. SHG band at 400 nm and a large fluorescence band are measured.

In Fig. 10 is presented the measured spectrum from an organic thin film (100 nm thick) sample. The laser source was the femosecond oscillator Tsumami at 80 MHz and 80 fs pulse duration. The spectrum is composed by a strong fluorescent band and a relatively small second harmonic band. Measuring the intensity of the fluorescence spectrum recorded in every point of the sample the specialized software can reconstruct a 2-Photon Excitated Fluorescence image, which could give information about the uniformity of distribution of the sample film on the silicon substrate.

8. CONCLUSIONS

In this paper we presented a complex but low cost microscope for laser processing and characterization. We demonstrated various experimental techniques using short laser pulses at pico and femtoseconds time duration. Direct-writing techniques such as laser ablation, two-photon photopolymerization, and LIFT, were used in order to produce microstructures on different material surfaces and in transparent materials. Nanostructuring was demonstrated by laser ablation in near-field regime using colloidal microspheres as focusing micro-optics. Features down to 100 nm were produced. Our microscope system is also configured for spectroscopic characterization by laser scanning with femtoseconds laser pulses. Two-photon excided emission can be recorded from various organic or non-organic samples.

Acknowledgements. This work was supported by CNCSIS – UEFISCSU, project number PNII – IDEI 268/2007, and CNMP project FEMAT nr. 11-030/2007.

REFERENCES

1. Horst-Günter Rubahn, *Laser Applications in Surface Science and Technology*, John Wiley & Sons 1999.
2. John F. Ready, *Industrial Applications of Lasers*, Academic Press, San Diego, 1997.
3. M.L. Wolbarsht, *Laser Applications in Medicine & Biology*, Plenum Press, New York, 1991.
4. Koji Sugioka, Michel Meunier, and Alberto Piqué, *Laser Precision Microfabrication*, Springer Series in Materials Science, Vol. 135, 2010.
5. D. R. S. Cumming, S. Thoms, S. P. Beaumont and J. M. R. Weaver, Appl. Phys. Lett., **68**, 322 (1996).
6. H. I. Smith and M.L. Schattenburg, IBM J. Res. Dev., **37**, 319 (1993).
7. C.W. Gwyn, R. Stulen, D. Sweeney, D. Attwood, *Extreme ultraviolet lithography*, J. Vac. Sci. Technol. **16**, 3142 (1998).
8. X. Liu, D. Du, and G. Mourou, IEEE J. Quantum Electron, **33**, 1706 (1997).
9. P.P. Pronko, SK. Dutta, J. Squier, J.V. Rudd, D. Du, G. Mourou, Opt. Comm., **114**, 106 (1995).
10. Julia Eizenkop, Ivan Avrutsky, Gregory Auner, Daniel G. Georgiev, and Vipin Chaudhary, J. Appl. Phys, **101**, 094301 (2007).
11. Z.B. Wang , B.S. Luk'yanchuk, L. Li, P.L. Crouse, Z. Liu, G. Dearden and K.G. Watkins, Appl. Phys. A: Materials Science & Processing, **89**, 363 (2007).
12. M. Zamfirescu, G. Sajin, A. Bunea, F. Craciunoiu, S. Simion, R. Dabu, J. Optoelectr. Adv. Mat., **12**, 686–691 (2010).
13. S. Maruo, O. Nakamura, and S. Kawata, Opt. Lett., **22**, 132 (1997).
14. S. Kawata, H. B. Sun, T. Tanaka, and K. Takada, Nature, **412**, 697 (2001).
15. T. Tanaka, H.-B. Sun, and S. Kawata, Appl. Phys. Lett., **80**, 312 (2002).
16. S. H. Park, S. H. Lee, D. Y. Yang, H. J. Kong, and K.-S. Lee, Appl. Phys. Lett., **87**, 154108 (2005).
17. J.Serbin, A. Ovsianikov, and B. Chichkov, Opt. Exp., **12**, 5221 (2004).
18. H.-B. Sun, T. Tanaka, and S. Kawatab, Phys. Lett., **80**, 3673 (2002).
19. M. Farsari, G. Filippidis, C. Fotakis. Optics Letters, **30**, 3180 (2005).
20. D. Tan, Y. Li, F. Qi, H. Yang, Q.Gong, X. Dong and X., Appl. Phys. Lett., **90**, 071106 (2007).
21. S.H. Park, T. W. Lim, D.-Y. Yanga, N. C. Cho and K.-S. Lee, Appl. Phys. Lett., **88**, 173133 (2006).
22. J. Bohandy, B. F. Kim, and F. J. Adrian, J. Appl. Phys., **60**, 1538 (1986).
23. I. Zergioti, S. Mailis, N. A. Vainos, C. Fotakis, S. Chen, C. P. Grigoropoulos App. Surf. Sci., **127–129**, 601–605 (1998).
24. M. Sanz, M. Walczak, M. Oujja, C. Domingo, A. Klini, E.L. Papadopoulou, C. Fotakis, M. Castillejo, Thin Solid Films, **518**, 5525–5529 (2010).
25. A. Piqué, R. C. Y. Auyeung, J. L. Stepnowski, D. W. Weir, C. B. Arnold, R. A. McGill, D. B. Chrisey, Surface and Coatings Technology, **163–164**, 293–299 (2003).
26. B.Thomas, A. P. Alloncle, P. Delaporte, M.Sentis, S.Sanaur, M.Barret, P. Collot, Applied Surface Science, **254**, 1206–1210 (2007).
27. F. Guillemot, A. Souquet, S. Catros, B. Guillotin, J. Lopez, M. Faucon, B. Pippenger, R. Bareille, M. Rémy, S. Bellance, P. Chabassier, J.C. Fricain, J. Amédée, Acta Biomaterialia, **6**, 2494–2500 (2010).
28. M. Colina, P. Serra, J.M. Fernández-Pradas, L. Sevilla, J.L. Morenza Biosensors and Bioelectronics, **20**, 1638–1642 (2005).

29. V. Dinca, E. Kasotakis, J. Catherine, A. Mourka, A. Mitraki, A. Popescu, M. Dinescu, M. Farsari, C. Fotakis, Appl. Surf. Sci., **254**, 1160–1163 (2007).
30. D. P. Banks, C. Grivas, J. D. Mills, R. W. Eason, and Ioanna Zergioti, Appl. Phys. Lett., **89**, 193107 (2006).
31. A. Piqué, S.A. Mathews, B. Pratap, R.C.Y. Auyeung, B.J. Karns, S. Lakeou, Microelectronic Engineering, **83**, 2527–2533 (2006).
32. D. W. Pohl, Philos. T. Roy. Soc. A, **362**, 701 (2004).
33. D. H. Lowndes, Adv. Mater. Process, **157**, 48 (2000).
34. A. Lewis, H. Taha, A. Strinkovski, A. Manevitch, A. Khatchatouriants, R. Dekhter and E. Ammann, Nat. Biotechnol., **21**, 1377 (2003).
35. D. W. Pohl and L. Novotny, J. Vac. Sci. Technol. B, **12**, 1441 (1994).
36. D. Richards, Philos. T.Roy. Soc. A, **361**, 2843 (2003).
37. Z.B. Wang, M.H. Hong, B.S. Luk'yanchuk, Y. Lin, Q.F. Wang, T.C. Chong, J. Appl. Phys., **96**, 6845 (2004).
38. S.M. Huang, M.H. Hong, B. Lukiyanchuk, T.C. Chong, Appl. Phys. A, **77**, 293 (2003).
39. M. Mosbacher, H.-J. Muenzer, J. Zimmermann, J. Solis, J. Boneberg, P. Leiderer, Appl. Phys. A, **72**, 41 (2001).
40. H.J. Munzer, M. Mosbacher, M. Bertsch, J. Zimmermann, P. Leiderer, J. Boneberg, J. Microsc., **202**, 129 (2000).
41. H. Takada, M. Obara, Jpn. J. Appl. Phys., **44**, 7993 (2005).
42. M. Ulmeanu, M. Zamfirescu, R. Medianu, Colloid Surface A, **338**, 87 (2009).
43. B. Huettner, G. C. Rohr, Applied Surface Science, **126**, 129 (1998).
44. W. Denk, K. R Delaney, A. Gelperin, D. Kleinfeld, B. W. Strowbridge, D. W.Tank, , R.Yuste, J. Neurosci. Methods, **54**, 151-162 (1994).
45. F. Helmchen, W. Denk, Curr. Opin. Neurobiol., **12**, *5*, 593–601 (2002).
46. P. J. Campagnola, M. Loew, Nature Biotechnology, **21**, 1356–1360 (2003).
47. H. Ernst Keller, *Objective Lenses for Confocal Microscopy*, Handbook of Biological Confocal Microscopy, ed. James B. Pawley, Plenum Press, NY, 1995.